Pure Electric and Magnetic Hotspots by Dielectric Cylindrical Dimers

Ali Mirzaei and Andrey Miroshnichenko
Nonlinear Physics Centre, Research School of Physics and Engineering
Australian National University, 59 Mills road, Acton, ACT 2601, Australia

Abstract— We analyze the near-field enhancement in dielectric nanowire dimers, using mode expansion analytical method and a genetic algorithm. We study the electric and magnetic hotspots and how they form in both TE and TM polarizations and compare them with plasmonic dimers, considering experimental data to describethe materials. We show that in dielectric dimers, two pure magnetic and electric hotspots can be achievable simultaneously in two sides of the dimer gap and with strength comparable to plasmonic dimers. We show that in plasmonic dimers these pure hotspots are closer and less distinguishable and in the opposite directions compared to dielectric dimers.

1. INTRODUCTION

Various structures have been reported to control the near-field behavior of light [1–3]. Near-field enhancement by localized plasmon polaritons is attracting more attentions to nanoplasmonics [4–8]. However, plasmonic structures suffer from strong dissipative losses in metallic components, even far from plasmonic resonances [9]. Recently, dielectric materials are investigated as competitive alternatives to plasmonic counterpart to reduce the dissipative losses [1]. At the same time, the ability to achieve such level of the near-field enhancement comparable with plasmonic nanostructures, is still a challenge [11–14]. To address this, we analyze and design optimal dimers configurations to achieve the strongest near-field enhancement in the visible regimes by using realistic experimental data of the materials [15, 16]. We demonstrate that by using dielectric materials, it is possible to create both electric and magnetic hotspots comparable with plasmonic structures in TE polarization (magnetic field parallel to the axis of nanowires). We also show the possibility to achieve near-field-enhancement in TM polarization with dielectrics nanowires, which is not possible by using metallic materials. Finally we introduce pure magnetic and electric hotspots both together simultaneously by using dielectric cylindrical dimers. In this work, despite of our previously done study [17], we will concentrate only on near field studies and add more in depth interpretations of hotspots forming.

2. METHODOLOGY

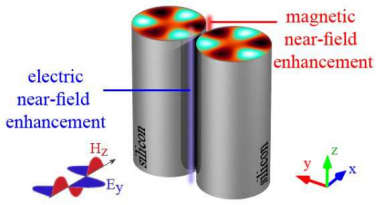

Figure 1: Schematic of a cylindrical dimer, incident planewave and the hotspots.

To simplify our analysis we focus on a symmetric dimer configuration as is shown in Fig. 1 and assume that the nanowires are made of the same material, with same diameter and also placed symmetrically around the origin [18]. Two-dimensional general arrangement of dimer's elements (nanowires) is shown in Fig. 2. The incident planewave is illuminating in the x direction with either TE or TM polarization. In TE polarization, the incident planewave can be written as $H^{inc} = H_0 e^{-i\omega t + i2\frac{\pi}{\lambda} r\cos(\varphi)}$, in which φ is the polar angle in cylindrical coordinate. We use the multipole expansion method to describe the interaction of light with nanowires [19, 20]. The total field of an individual nanowire can then be presented as [21]:

$$H^l_{total} = H_0 e^{-i\omega t} \sum_{n=-\infty}^{+\infty} e^{in(\varphi+\frac{\pi}{2})} \left[\tau^l_n J_n(\beta_l r) + \rho^l_n H^{(1)}_n(\beta_l r)\right], \quad (1)$$

where $\beta_l = \frac{2\pi}{\lambda}\sqrt{\varepsilon_l(\lambda)}$, H_0 is the incident planewave amplitude, J_n and $H_n^{(1)}$ are the n'th order Bessel and Hankel functions of the first kind, respectively; n is the mode number, l is the number of layer which is 1 for the nanowires material and 2 for the surrounding material which is air, $\varepsilon_l(\lambda)$ is the dielectric constant of the l'th layer at wavelength λ and r is the radius. For TM polarization, an expression similar to Eq. (1) can be written for E^l_{total}. Also the size-dependent effect of plasmonic layers has been taken into account [22, 23].

By solving the boundary condition equations in $r = R$ and for individual wires separately, first we obtain the expansion coefficients, τ_n^l and ρ_n^l [20, 21]. Then we employ multiple scattering problem solution, to consider the interaction between the nanowires [19, 24, 25]. Using the translation additional theorem [26]. In this case, the scattered field from one cylinder becomes an incident wave on another in addition to the incident planewave. This procedure leads the modified expansion coefficients ρ_n^{air} and consequently τ_n^l of each nanowire.

Then, we search for the optimized parameters to maximize the fields amplitude in the middle of the dimer's gap to form enhanced hotspots using a genetic algorithm (GA) [27] we have developed for electromagnetic optimization [28, 29]. We define a fitness function in the middle of the gap as is described in [17].

3. RESULTS AND DISCUSSION

Silicon and silver as two commonly used dielectric and plasmonic materials have been chosen here to provide a competitive analysis of dimer structures. We analyze two different directions of the dimer's axis, parallel and perpendicular to the direction of the incident plane wave propagation. The last row of Table 1 illustrates the optimization results by using the optimized radius, gap size, and the wavelength which are shown in the previous rows for electric and magnetic hotspots in both orientations. The summary of the optimization results and the position of the electric and magnetic hotspots is also demonstrated schematically in Fig. 2. The results reveal that for TE polarization, electric and magnetic hotspots are achievable with almost lossless dielectric dimers, comparable with plasmonic ones. The results also show that for TM polarization, it is possible to obtain strong hotspots by dielectric dimers, which is not possible using plasmonic materials. Our study shows that the hotspots are not exactly in the middle of the gap in perpendicular arrangement. In particular, Fig. 2(a) shows that in dielectric dimers, the location of the magnetic hotspot is shifted toward $+x$ direction, in respect to the middle of the gap (the same as Fig. 2(e)). The electric hotspot in this dimer is shifted in the opposite direction. It is interesting to note, that the shifts of the location of the hotspots in plasmonic dimers are reversed, as can be seen from Fig. 2(c). However, the amount of these shifts in plasmonic dimers are smaller and the two hotspots have overlapped fields in the middle.

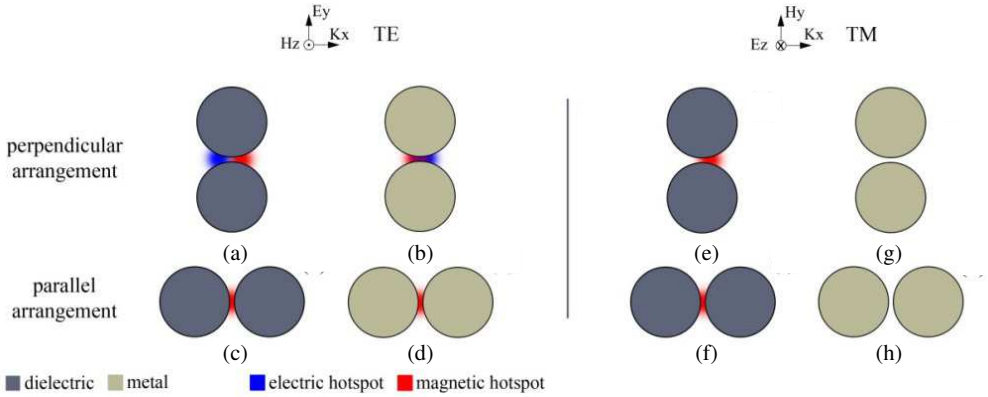

Figure 2: Schematic near-field hotspots excitation in dielectric and metallic dimers. Panel (a) demonstrates that for dielectric nanowires, it is possible to separate magnetic and electric hotspots. The small shift of hotspots' location from the centre of the gap is demonstrated in panels (a), (e). The shift becomes smaller with almost overlapped magnetic and electric hotspots in the plasmonic case, as demonstrated in panel (c). Panels (a), (c), (e) show that the direction of the locational displacements of magnetic and electric hotspots are opposite in dielectric and plasmonic dimers. Note here, that such hotspots do not exist for TM polarization in metallic nanowires.

Table 1: Optimization results for the electric and magnetic hotspots in the middle of the gap in dimers with their axis perpendicular/parallel to the direction of the incident planewave. The optimized field values are normalized to the corresponding H_0 or E_0 values. In all our calculations the first 30 modes have been taken into account.

	perpendicular								parallel							
Mat.	Si				Ag				Si				Ag			
Pol.	TE		TM		TE		TM		TE		TM		TE		TM	
Param.	$\|Hz\|$	$\|Et\|$	$\|Ez\|$	$\|Ht\|$	$\|Hz\|$	$\|Et\|$	$\|Ez\|$	$\|Ht\|$	$\|Hz\|$	$\|Et\|$	$\|Ez\|$	$\|Ht\|$	$\|Hz\|$	$\|Et\|$	$\|Ez\|$	$\|Ht\|$
λ	626	613	579	615	806	432	318	306	634	650	634	554	477	330	324	310
R	121	151	51	89	200	57	10	16	84	133	93	28	55	20	20	20
Gap	3	3	3	3	3	3	20	17	3	3	3	3.1	3	7.8	40	3.1
Optm. value	8.1	17.9	2.2	9.6	9.3	20.4	0.9	1	6.2	2	2.6	8.5	7.7	1.6	0.9	1

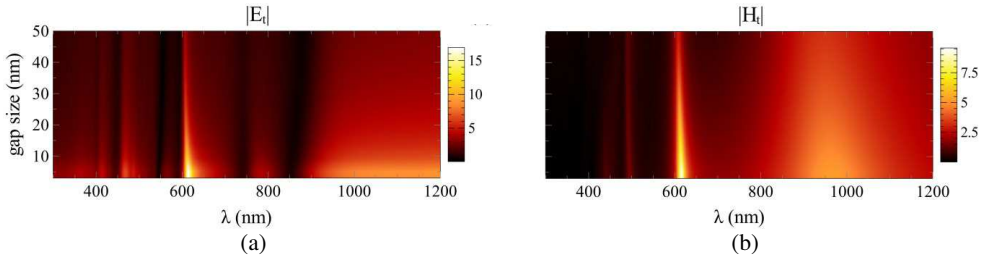

Figure 3: Spectral variation of absolute value of the fields in the middle of the gap by changing the gap size in twodifferentsilicondimersbased on (a) column 2 and (b) column 4 of Table 1.

To have a better understanding of the hotspots behaviour, the dependancy of the hotspots to the gap size has been plotted in a wide spectral range in Fig. 3. Both dimers show considerable field enhancement around 614 nm which stay almost enhanced by increasing the gap size. Here we noe that the dimers can be optimized to creat hotspots at any wavelength but the results in Table 1, demonstrate the best parameters value we could obtain. Dark and bright areas in Fig. 3. Reveal that changing the gap size does not considerably affect the spectral behaviour of the hotspots.

Now we analyse the local shifts of hotspotsin both dielectric and plasmonic dimers, presented in Figs. 2(a), (c), (e). All three figures indicate that the local shift of magnetic and electric hotspots are opposite for dielectric and plasmonic dimers independent of the polarization. Here we plot the field profile of two different dimers with optimized electric and magnetic hotspots with TE and TM polarizations in Fig. 4. The parameters for dielectric and plasmonic dimers can be found in the Table 1 in the second and fourth columns, respectively. In spite of plasmonic dimers, in dielectric structures the magnetic field intends to remain mainly inside the nanowires. Fig. 4 demonstrates that the maximum of the absolute value of the fields is more than the optimized results in the Table 1 which presents values in the middle of the gap. Figs. 4(a) and (b) show the electric and magnetic hotspots for two different silicon dimers, based on the results in columns two and four of Table 1, respectively. Similarly, Figs. 4(d) and (e) show the electric and magnetic hotspots for two different silver dimers, based on the results in columns six and five of the Table, respectively. In Figs. 4(c) and (f) we show the exact location of the hotspots and the field distribution around it, along the line perpendicular to the dimer's axis passing through the centre of the gap. Comparison between Figs. 4(c) and (f) reveals that the amounts of the local shifts of the hotspots from the centre of the gap are much less in plasmonic dimers compare to dielectric ones.

The results shown in Figs. 4(c) and (f) reveal another interesting fact that the electric field becomes near zero in a region close to the electric hotspot, making two maximized and minimized electric field strength points close to each other. This becomes more interesting in the case of dielectric dimers, where this zero electric field point, overlaps the magnetic hotspot. This means that the magnetic hotspot in dielectric cylindrical dimers, is pure magnetic. Fig. 5 compares the electric and magnetic field profiles in the dimer shown in Fig. 4(a) which also demonstrates a similar pure electric hotspot with near zero magnetic field.

To have a dipper insight to the origin of how these hotspots are formed, we present modes decomposition of the dimer and analyse the dominant mode contribution to the formation of the

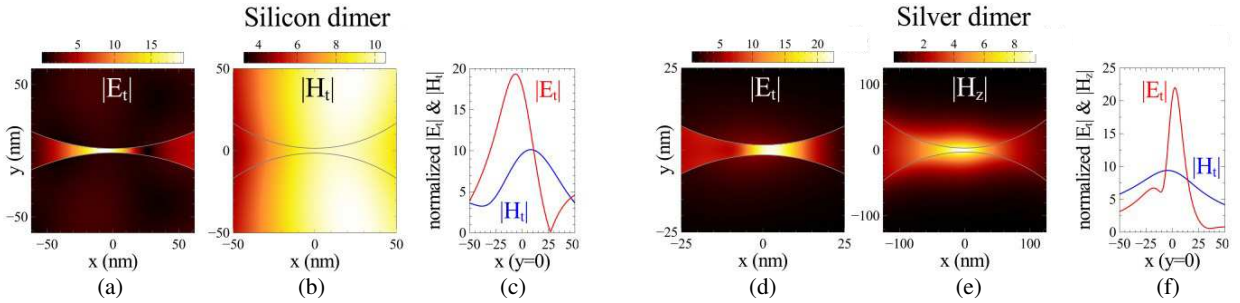

Figure 4: The field profile of two different silicon dimers optimized for their (a) electric and (b) magnetic hotspots, based on the results in the second and fourth columns of Table 1 respectively. Fig. 4(c) shows the fields distribution along the x axis, and the location of the hotspots in the structures of Figs. 4(a) and (b). The incident planewave is illuminating in x direction and the fields value are normalized with respect to the absolute value of the incident fields. Similar results are shown for two different silver dimers in Fig. 4(d) to (f).

corresponding hotspots, which are created by interference of different overlapping harmonics. In Fig. 5 we show the real part of the magnetic field profile of the first four harmonics in the same silicon dimer, with perpendicular propagation. As a result of the symmetrical incidence, the expansion coefficients ρ_n^l of one cylinder are equal to ρ_{-n}^l of the other one, which confirms the theory that the cylinders are practically indistinguishable in broadside illumination. Fig. 5 demonstrates how the superposition of the different modes forms the total field profile with no symmetry with respect to the centre of the gap in x direction, resulting magnetic bright and dark spots shifted from the centre of the gap. In other words, destructive and constructive effects of different harmonics of the scattered and incident fields, make it possible to engineer the magnetic hot and cold spots in two sides of the gap. The map of the electric filed modes' distribution also shows the similar results but in the opposite direction. Consequently, by overlapping the electric and magnetic hotspots on the other field's dark area, both pure magnetic and pure electric hotspots are formed as is demonstrated in Fig. 5. Here we note that the above investigated silicon dimer is optimized for the electric near field enhancement, based on the descriptions in column two of Table 1, which indicates that the behaviour of the resulting magnetic hotspot is not necessarily optimal.

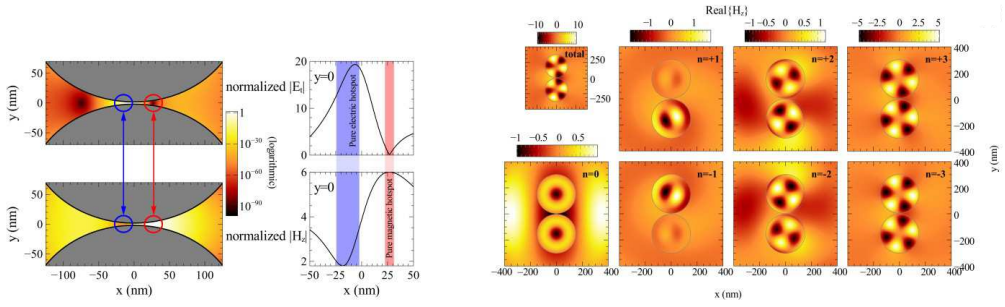

Figure 5: The hotspots in the silicon dimer shown in Fig. 4(a) based on column two of Table 1, with plane wave illuminating from left. (a) Compares the locations of the hotspots and demonstrates their electric and magnetic purity (The fields' amplitude values are normalized to those of the incident wave). (b) The real part of magnetic field profile of the dimer. The field amplitude for modes n>3 becomes negligible. The expansion coefficient ρ_n^l of one cylinder is equal to ρ_{-n}^l of the other one. The dimer is optimized for its electric hotspot but the magnetic field is plotted instead of the electric one which is much weaker than magnetic field inside the structure.

4. CONCLUSION

We studied dielectric/plasmonic nanowire dimers, with two parallel/perpendicular dimer configurations with respect to the direction of the incident wave propagation. We analysed both electric/magnetic hotspots and their different harmonics in both TE/TM polarizations. The displacement of the hotspots from the centre of the gap is also analysed in details. We showed that for

electric/magnetic hotspots in dielectric dimers, there is a point on the other side of the gap with zero amplitude of the same field (electric/magnetic), which overlaps the hotspot of the other field (magnetic/electric). This leads to formation of both pure magnetic and electric hotspots in opposite sides of the gap. All the results are achieved analytically by multipole expansion method using the first 30 harmonics. The optimized designs have been also presented for all the cases separately using a genetic algorithm. These results offer new approaches for near-field engineering of variety of applications.

REFERENCES

1. Rahmani, M., E. Yoxall, B. Hopkins, Y. Sonnefraud, Y. Kivshar, M. Hong, C. Phillips, S. A. Maier, and A. E. Miroshnichenko, "Plasmonic nanoclusters with rotational symmetry: Polarization-invariant far-field response vs changing near-field distribution," *ACS Nano*, Vol. 7, No. 12, 11138–11146, 2013.
2. Miroshnichenko, A. and Y. Kivshar, "Fano resonances in all-dielectric oligomers," *Nano Lett.*, Vol. 12, No. 12, 6459–6463, 2012.
3. Filonov, D., A. Slobozhanyuk, A. Krasnok, P. Belov, E. Nenasheva, B. Hopkins, A. Miroshnichenko, and Y. Kivshar, "Near-fieldmapping of Fano resonances in all-dielectricoligomers," *Appl. Phys. Lett.*, Vol. 104, 021104, 2014.
4. Siegfried, T., Y. Ekinci, O. Martin, and H. Sigg, "Gap plasmons and near-field enhancement in closely packed sub-10 nm gap resonators," *Nano Lett.*, Vol. 13, No. 11, 5449–5453, 2013.
5. Dodson, S., M. Haggui, R. Bachelot, J. Plain, S. Li, and Q. Xiong, "Optimizing electromagnetic hotspots in plasmonic bowtie nanoantennae," *J. Phys. Chem. Lett.*, Vol. 4, No. 3, 496–501, 2013.
6. Aouani, H., M. Rahmani, H. Sipova, V. Torres, K. Hegnerova, M. Beruete, J. Homola, M. Hong, M. Navarro-Cía, and S. Maier, "Plasmonic nanoantennas for multispectral surface-enhanced spectroscopies," *J. Phys. Chem. C*, Vol. 117, No. 36, 18620–18626, 2013.
7. Rahmani, M., A. Miroshnichenko, D. Lei, B. Luk'yanchuk, M. Tribelsky, A. Kuznetsov, Y. Kivshar, Y. Francescato, V. Giannini, M. Hong, and S. Maier, "Beyond the hybridization-effects in plasmonic nanoclusters: Diffraction-induced enhanced absorption and scattering," *Small*, Vol. 10, No. 3, 576–583, 2013.
8. Yang, J., M. Rahmani, J. Teng, and M. Hong, "Magnetic-electricinterference in metal-dielectric-metaloligomers: Generation of magneto-electric Fano resonance," *Opt. Mat. Express*, Vol. 2, No. 10, 1407–1415, 2012.
9. Maier, S., *Plasmonics: Fundamentals and Applications*, Springer, 2007.
10. Bakker, R., D. Permyakov, Y. Yu, D. Markovich, R. Dominguez, L. Gonzaga, A. Samusev, Y. Kivshar, B. Luk'yanchuk, and A. Kuznetsov, "Magnetic and electric hotspots with silicon nanodimers," *Nano Lett.*, Vol. 15, No. 3, 2137–2142, 2015.
11. Sigalas, M., D. Fattal, R. Williams, S. Wang, and R. Beausoleil, "Electric field enhancement between two Si microdisks," *Opt. Express*, Vol. 15, No. 22, 14711–14716, 2007.
12. Laroche, M., S. Albaladejo, R. Carminati, and J. Saenz, "Optical resonances in one-dimensional dielectric nanorod arrays: Field-induced fluorescence enhancement," *Opt. Lett.*, Vol. 32, No. 18, 2762–2764, 2007.
13. Albella, P., M. Poyli, M. Schmidt, S. Maier, F. Moreno, J. Saenz, and J. Aizpurua, "Low-loss electric and magnetic field-enhanced spectroscopy with subwavelength silicon dimers," *J. Phys. Chem. C*, Vol. 117, No. 26, 13573–13584, 2013.
14. Boudarham, G., R. Abdeddaim, and N. Bonod, "Enhancing the magnetic field intensity with a dielectric gap antenna," *App. Phys. Lett.*, Vol. 104, 021117, 2014.
15. Palik, E., *Handbook of Optical Constants of Solids*, Academic Press, 1998.
16. Aspnes, D. and A. Studna, "Dielectric functions and opticalparameters of Si, Ge, GaP, GaAs, GaSb, InP, InAs, and InSb from 1.5 to 6.0 eV," *Phys. Rev. B*, Vol. 27, No. 2, 985–1009, 1983.
17. Mirzaei, A. and A. Miroshnichenko, "Electric and magnetichotspots in dielectricnanowired-imers," *Nanoscale*, Vol. 7, 5963–5968, 2015.
18. Tsuei, T. and P. Barber, "Multiple scattering by twoparalleldielectriccylinders," *App. Optics*, Vol. 27, No. 16, 3375–3381, 1988.
19. Balanis, C., *Advanced Engineering Electromagnetics*, Wiley, 1998.
20. Schachter, L., *Beam-Wave Interaction in Periodic and Quasi-Periodic Structures*, Springer, 2011.

21. Mirzaei, A., A. Miroshnichenko, N. Zharova, and I. Shadrivov, "Light scattering by nonlinear cylindrical multilayer structures," *J. Opt. Soc. Am. B*, Vol. 31, No. 7, 1595–1599, 2014.
22. Kreibig, U., "Electronicproperties of smallsilverparticles: The optical constants and their temperature dependence," *J. Phys. F: Metal. Phys.*, Vol. 4, No. 7, 999–1014, 1974.
23. Mirzaei, A., I. Shadrivov, A. Miroshnichenko, and Y. Kivshar, "Cloaking and enhancedscattering of core-shell plasmonic nanowires," *Opt. Express*, Vol. 21, No. 9, 10454–10459, 2013.
24. Olaofe, G., "Scattering by two cylinders," *Radio Sci.*, Vol. 5, No. 11, 1351–1360, 1970.
25. Quinten, M., *Optical Properties of Nanoparticle Systems: Mie and Beyond*, J. Wiley, 2010.
26. Watson, G., *A Treatise on the Theory of Bessel Functions*, University Press, 1966.
27. Mitchell, M., *An Introduction to Genetic Algorithms*, MIT Press, 1966.
28. Mirzaei, A., A. Miroshnichenko, I. Shadrivov, and Y. Kivshar, "Superscattering of light optimized by a geneticalgorithm," *Appl. Phys. Lett.*, Vol. 105, 011109, 2014.
29. Mirzaei, A., A. Miroshnichenko, I. Shadrivov, and Y. Kivshar, "All-dielectric multilayer cylindrical structures for invisibility cloaking," *Sci. Reports*, Vol. 5, 9574, 2015.
30. Zhu, W. and K. Crozier, "Quantum mechanicallimit to plasmonic enhancement as observed by surface-enhanced Raman scattering," *Nat. Comm.*, Vol. 5, 5228, 2014.